Korean J. Chem. Eng., **29**(12), 1688-1694 (2012)
DOI: 10.1007/s11814-012-0091-3

Onset of radial viscous fingering in a Hele-Shaw cell

Min Chan Kim†

Department of Chemical Engineering, Jeju National University, Jeju 690-756, Korea
(*Received 27 March 2012 • accepted 7 June 2012*)

Abstract−The onset of viscous fingering in a radial Hele-Shaw cell was analyzed by using linear theory. In the self-similar domain, the stability equations were derived under the normal mode analysis. The resulting stability equations were solved analytically by expanding the disturbances as a series of orthogonal functions and also numerically by employing the shooting method. It was found that the long wave mode of disturbances has a negative growth rate and the related system is always stable. For the limiting case of the infinite Péclet number, $Pe\rightarrow\infty$, the analytically obtained critical conditions are $R_c=11.10/\sqrt{Pe}$ and $n_c=0.87\sqrt{Pe}$. For $Pe\geq100$, these stability conditions explain the system quite well.

Key words: Viscous Fingering, Radial Flow, Hele-Shaw Cell, Spectral Analysis, Numerical Shooting Method

INTRODUCTION

The instability during the displacement of two-miscible fluids in a porous medium was first studied experimentally by Hill [1]. If the displacing fluid is less viscous than the displaced one, this unfavorable viscosity difference makes the system unstable and causes the displacing fluid to channel through the displaced one. Recently, Holloway and de Bruyn [2,3] showed experimentally that similar fingering can occur in a single fluid saturated within the Hele-Shaw cell. In their experiments, the viscosity contrast is induced by the temperature difference.

The viscous fingering occurring in radial source flows has attracted many researchers' interests (see Tan and Homsy [4], Yortsos [5] and the references given therein). Later, Riaz and Meiburg [6,7] and Riaz et al. [8] extended this problem by considering various effects such as 3-dimensional disturbances, velocity-induced dispersion and concentration-dependent diffusion. They solved the stability problem with the linear stability theory and direct numerical simulation. Pritchard [9] revisited this problem by considering double diffusive effects due to the heat and mass transfer. He expanded the temperature and concentration disturbances as a series of orthogonal functions. Recently, Kim [10] proved that in the limiting case of infinite Péclet number, the principle of the exchange of stabilities is valid.

Even though the above studies gave the growth rate of fingering instability, less attention has been given on the critical conditions of the onset of instability. In the present study, the onset of viscous fingering of the radial source flow in a Hele-Shaw cell is analyzed under linear theory. Under the normal mode analysis the onset and the growth of the azimuthal instability are analyzed theoretically by using the spectral approach and numerically by employing numerical shooting method. Based on a more robust mathematical basis, the present complements the previous results from the numerical solution.

†To whom correspondence should be addressed.
E-mail: kim.minchan@gmail.com

GOVERNING EQUATIONS AND BASE FIELDS

The pseudo two-dimensional flow that results from the injection of fluid into a horizontal radial Hele-Shaw cell, whose thickness is b, from a line source at position $\bar{r}=0$ with a constant areal flux Q and the temperature T_H is considered here. The viscosity of the displacing fluid is μ_H and that of the ambient displaced one is μ_C where the temperature is T_C. Fig. 1 illustrates the present system schematically. Under the Hele-Shaw approximation, the dimensionless governing equation in the cylindrical (r, ϕ)-coordinate can be written as,

$$\frac{1}{r}\frac{\partial}{\partial r}(ru)+\frac{1}{r}\frac{\partial v}{\partial \phi}=0, \tag{1}$$

$$\frac{1}{12}\frac{\partial p}{\partial r}=-\mu u, \tag{2}$$

$$\frac{1}{12}\frac{1}{r}\frac{\partial p}{\partial \theta}=-\mu v, \tag{3}$$

$$\frac{\partial \theta}{\partial \tau}+\left[\frac{1}{r}\frac{\partial(ru\theta)}{\partial r}+\frac{1}{r}\frac{\partial(v\theta)}{\partial \phi}\right]=\frac{1}{Pe}\left[\frac{1}{r}\frac{\partial}{\partial r}\left(r\frac{\partial \theta}{\partial r}\right)+\frac{1}{r^2}\frac{\partial^2\theta}{\partial \phi^2}\right], \tag{4}$$

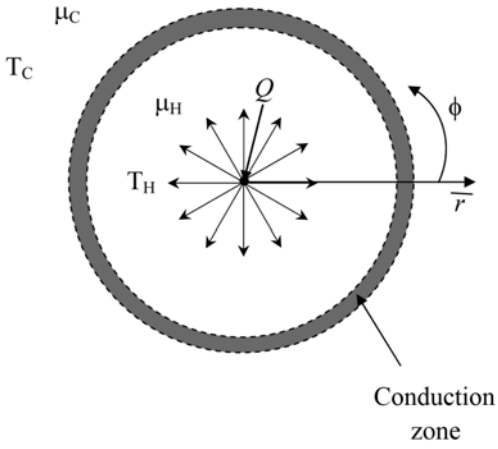

Fig. 1. Schematic diagram of system considered here.

where b, b^2/Q, Q/b, μ_H, $\mu_H Q/b^2$ and $\Delta T(=T_H-T_C)$ are used as length, time, velocity, viscosity, pressure and temperature scales, respectively. Here, the important parameter Péclet number, Pe, is defined as [6,7]

$$\mathrm{Pe}=\frac{Q}{\kappa}, \tag{5}$$

where κ is the thermal diffusivity. The Péclet number means the ratio of the convective transfer rate and conductive one. It is well-known that the conductive term makes the convective motion stable, which will be discussed later, and therefore, higher values of the Péclet number promote instability. Holloway and de Bruyn [2,3] conducted systematic experiments on the radial viscous fingering in a Hele-Shaw cell. According to their experimental data, the Péclet number for the miscible case ranges from 10^3 to 10^5. Thus, high Pe is common in experimental situations. Another parameter for the instabilities is the viscosity variation with the temperature and its relation is assumed to be

$$\mathrm{R}=-\frac{1}{\mu}\frac{\partial\mu}{\partial\theta}=\text{constant}. \tag{6}$$

Holloway and de Bruyn [2,3] suggested the temperature-dependent viscosity as

$$\mu=\exp(a_0-a_1T+a_2T^2). \tag{7}$$

And, they defined the viscosity contrast as

$$\mathrm{M}=\frac{\mu(T_C)}{\mu(T_H)}=\exp\{a_1\Delta T+a_2\Delta T(T_H+T_C)\}. \tag{8}$$

Since $\theta\leq 1<<(T_H+T_C)/\Delta T$ is guaranteed in their experiments, the following relation between M and R can be used:

$$\mathrm{M}\approx\exp(\mathrm{R}), \tag{9}$$

Since viscous fingering is driven by the viscosity gradient, which is quantified by R, the fingering instability can never be expected for R=0. However, even though there is a significant viscosity mismatch, the system can remain stable if there is no flow, i.e., Pe=0. This means that the stability of the present system is controlled by both Pe and R not Pe or R alone.

For a constant flux injection system, where $u_0=1/r$, the axisymmetric base temperature is governed by [9],

$$\frac{\partial\theta_0}{\partial\tau}+\frac{1}{r}\frac{\partial\theta_0}{\partial r}\left(1-\frac{1}{\mathrm{Pe}}\right)=\frac{1}{\mathrm{Pe}}\frac{\partial^2\theta_0}{\partial r^2}, \tag{10}$$

under the following conditions:

$$\theta_0=1 \text{ at } r=0, \tag{11a}$$
$$\theta_0\to 0 \text{ as } r\to\infty. \tag{11b}$$

The above equation has the following similarity solution:

$$\theta_0(\xi)=\frac{\Gamma(\mathrm{Pe}/2,\xi)}{\Gamma(\mathrm{Pe}/2)}, \tag{12}$$

where $\theta_0=(T-T_C)/\Delta T$ is the dimensionless base temperature, $\xi=\mathrm{Pe}\,r^2/(4\tau)$ is the similarity variable, $\Gamma(\alpha,x)=\int_x^\infty t^{\alpha-1}\exp(-t)dt$ is the incomplete gamma function and the function $\Gamma(\alpha)$ is the gamma function. For the limiting case of $\mathrm{Pe}\to\infty$, the above temperature field reduces to

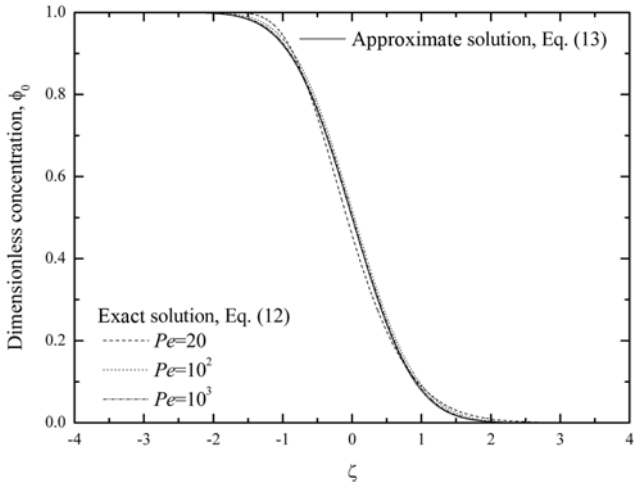

Fig. 2. Comparison of base temperature distributions of the various Pe.

$$\theta_0(\eta)=\frac{1}{2}\mathrm{erfc}(\eta), \tag{13}$$

where $\eta=(\xi-\mathrm{Pe}/2)/\sqrt{\mathrm{Pe}}$ and $\eta=0$ is the displacing front. As shown in Fig. 2, for $\mathrm{Pe}\geq 100$ the above solution approximates the exact one quite well.

LINEAR STABILITY THEORY

Under linear theory, the following linear stability equations can be obtained by perturbing Eqs. (1)-(4) [9]:

$$\frac{1}{r}\frac{\partial}{\partial r}(ru_1)+\frac{1}{r}\frac{\partial v_1}{\partial\phi}=0, \tag{14}$$

$$\frac{\partial p_1}{\partial r}=-\mu u_1-\frac{1}{r}\frac{d\mu}{d\theta}\theta_1, \tag{15}$$

$$\frac{1}{r}\frac{\partial p_1}{\partial\phi}=-\mu v_1, \tag{16}$$

$$\frac{\partial\theta_1}{\partial\tau}+\frac{1}{r}\frac{\partial\theta_1}{\partial r}+\frac{\partial\theta_0}{\partial r}u_1=\frac{1}{\mathrm{Pe}}\left[\frac{1}{r}\frac{\partial}{\partial r}\left(r\frac{\partial\theta_1}{\partial r}\right)+\frac{1}{r^2}\frac{\partial^2\theta_1}{\partial\phi^2}\right]. \tag{17}$$

The corresponding boundary conditions are

$$ru_1\to 0 \text{ and } \theta_1\to 0 \text{ as } r\to 0, \tag{18a}$$
$$u_1\to 0 \text{ and } \theta_1\to 0 \text{ as } r\to\infty. \tag{18b}$$

Here the subscripts '0' and '1' mean the base and disturbance quantities, respectively. Eliminating the pressure terms, the linear stability Eqs. (14)-(16) reduce to

$$\frac{\partial^2(ru_1)}{\partial r^2}+\left(\frac{1}{r}-\mathrm{R}\frac{\partial\theta_0}{\partial r}\right)\frac{\partial(ru_1)}{\partial r}+\frac{1}{r^2}\frac{\partial^2}{\partial\phi^2}(ru_1)=\mathrm{R}\frac{1}{r^2}\frac{\partial^2\theta_1}{\partial\phi^2}, \tag{19}$$

Using the similarity variable $\xi[=\mathrm{Pe}\,r^2/(4\tau)]$, Eqs. (17) and (19) are transformed into

$$\xi\frac{\partial^2(ru_1)}{\partial\xi^2}+\left(1-\mathrm{R}\frac{d\theta_0}{d\xi}\xi\right)\frac{\partial(ru_1)}{\partial\xi}+\frac{1}{4\xi}\frac{\partial^2(ru_1)}{\partial\phi^2}=\frac{1}{4\xi}\mathrm{R}\frac{\partial^2\theta_1}{\partial\phi^2}, \tag{20}$$

$$\tau\frac{\partial\theta_1}{\partial\tau}=\left[\xi\frac{\partial^2}{\partial\xi^2}+\left\{\xi+\left(1-\frac{\mathrm{Pe}}{2}\right)\right\}\frac{\partial}{\partial\xi}\right]\theta_1+\frac{1}{4\xi}\frac{\partial^2\theta_1}{\partial\phi^2}-\frac{1}{2}\mathrm{Pe}\frac{\mathrm{d}\theta_0}{\mathrm{d}\xi}(\mathrm{ru}_1), \quad (21)$$

$$\frac{\mathrm{d}\theta_0}{\mathrm{d}\xi}=-\frac{1}{\Gamma(\mathrm{Pe}/2)}\xi^{(Pe/2-1)}\exp(-\xi). \quad (22)$$

The corresponding boundary conditions are

$$\mathrm{ru}_1=\theta_1=0 \text{ as } \xi\to 0 \text{ and } \xi\to\infty. \quad (23)$$

For high Pe case, using $\eta=(\xi-\mathrm{Pe}/2)/\sqrt{\mathrm{Pe}}$, the above stability equations are approximated as

$$\left[\frac{\partial^2}{\partial\eta^2}+\mathrm{R}\frac{\partial\theta_0}{\partial\eta}\frac{\partial}{\partial\eta}+\frac{1}{\mathrm{Pe}}\frac{\partial^2}{\partial\phi^2}\right](\mathrm{ru}_1)=\mathrm{R}\frac{1}{\mathrm{Pe}}\frac{\partial^2\theta_1}{\partial\phi^2}. \quad (24)$$

$$\tau\frac{\partial\theta_1}{\partial\tau}=\frac{1}{2}\left[\frac{\partial^2}{\partial\eta^2}+2\eta\frac{\partial}{\partial\eta}+\frac{1}{\mathrm{Pe}}\frac{\partial^2}{\partial\phi^2}\right]\theta_1-\frac{1}{2}\frac{\partial\theta_0}{\partial\eta}\sqrt{\mathrm{Pe}}(\mathrm{ru}_1), \quad (25)$$

$$\frac{\mathrm{d}\theta_0}{\mathrm{d}\eta}=-\frac{1}{\sqrt{\pi}}\exp(-\eta^2). \quad (26)$$

under the following boundary conditions:

$$\mathrm{ru}_1=\theta_1=0 \text{ at } \eta=-\sqrt{\mathrm{Pe}}/2, \quad (27a)$$

$$\mathrm{ru}_1\to 0 \text{ and } \theta_1\to 0 \text{ as } \eta\to\infty \quad (27b)$$

NORMAL MODE ANALYSIS

As discussed by Tan and Homsy [4], one of major differences between the present radial flow system and the rectilinear one is that normal mode analysis is possible in the present radial fingering problem. Since the coefficients of the above equations are independent of ϕ and τ under the normal mode analysis, the disturbance quantities can be represented as

$$[\mathrm{ru}_1,\ \theta_1]=[\Psi(\xi),\ \Theta(\xi)]\exp(\mathrm{in}\phi)\tau^{\sigma}, \quad (28)$$

where n is the azimuthal wavenumber and the growth rate σ defined as

$$\tau\frac{\partial\theta_1}{\partial\tau}=\sigma\theta_1, \quad (29)$$

can be used for the stability measure. From Eqs. (20)-(23) and (28), the following stability equations can be obtained

$$\xi\frac{\mathrm{d}^2\Psi}{\mathrm{d}\xi^2}+\left(1+\frac{\mathrm{R}}{\Gamma(\mathrm{Pe}/2)}\xi^{(Pe/2-1)}\exp(-\xi)\xi\right)\frac{\mathrm{d}\Psi}{\mathrm{d}\xi}-\frac{\mathrm{n}^2}{4\xi}\Psi=-\frac{\mathrm{n}^2}{4\xi}\mathrm{R}\Theta, \quad (30)$$

$$\sigma\Theta=\left[\xi\frac{\mathrm{d}^2}{\mathrm{d}\xi^2}+\left\{\xi+\left(1-\frac{\mathrm{Pe}}{2}\right)\right\}\frac{\mathrm{d}}{\mathrm{d}\xi}\right]\Theta-\frac{\mathrm{n}^2}{4\xi}\Theta+\frac{1}{2}\frac{\mathrm{Pe}}{\Gamma(\mathrm{Pe}/2)}\xi^{(Pe/2-1)}\exp(-\xi)\Psi, \quad (31)$$

under the following boundary conditions:

$$\Psi=\Theta=0 \text{ as } \xi\to 0 \text{ and } \xi\to\infty. \quad (32)$$

For high Pe case, from Eq. (24)-(27), the above stability equations are approximated as

$$\frac{\mathrm{d}^2\Psi^*}{\mathrm{d}\eta^2}+\frac{\mathrm{R}}{\sqrt{\pi}}\exp(-\eta^2)\frac{\mathrm{d}\Psi^*}{\mathrm{d}\eta}-\mathrm{a}^2\Psi=\mathrm{a}^2\mathrm{R}^*\Theta. \quad (33)$$

$$\sigma\Theta=\frac{1}{2}\left[\frac{\mathrm{d}^2}{\mathrm{d}\eta^2}+2\eta\frac{\mathrm{d}}{\mathrm{d}\eta}-\mathrm{a}^2\right]\Theta+\frac{1}{2\sqrt{\pi}}\exp(-\eta^2)\Psi^*, \quad (34)$$

under the following boundary conditions

$$\Phi\to 0 \text{ and } \Psi^*\to 0 \text{ as } \eta\to\pm\infty, \quad (35)$$

where $\Psi^*=\sqrt{\mathrm{Pe}}\,\Psi$, $\mathrm{a}(=\mathrm{n}/\sqrt{\mathrm{Pe}})$ and $\mathrm{R}^*(=\mathrm{R}\sqrt{\mathrm{Pe}})$.

SOLUTION METHODS

1. Spectral Analysis

To analyze Eqs. (30)-(31), according to the Sturm-Liouville theory, let Θ as

$$\Theta(\xi)=\sum_{i=0}^{\infty}\mathrm{A}_i\mathrm{f}_i(\xi). \quad (36)$$

Here $\mathrm{f}_i(\xi)$ is the eigenfunction of the following Sturm-Liouville equation:

$$\left[\xi\frac{\mathrm{d}^2}{\mathrm{d}\xi^2}+\left\{\xi+\left(1-\frac{\mathrm{Pe}}{2}\right)\right\}\frac{\mathrm{d}}{\mathrm{d}\xi}\right]\mathrm{f}_i=-\lambda_i\mathrm{f}_i, \quad (37)$$

where λ_i is the eigenvalue corresponding to the eigenfunction $\mathrm{f}_i(\xi)$. Now, $\mathrm{f}_i(\xi)$ will be found in the following form:

$$\mathrm{f}_i(\xi)=\alpha_i\exp(-\xi)\xi^{Pe/2}\mathrm{g}_i(\xi). \quad (38)$$

By substituting the above form into Eq. (37), the following equation can be derived:

$$\xi\frac{\mathrm{d}^2\mathrm{g}_i}{\mathrm{d}\xi^2}+\left[\left(1+\frac{\mathrm{Pe}}{2}\right)-\xi\right]\frac{\mathrm{d}\mathrm{g}_i}{\mathrm{d}\xi}=-(\lambda_i-1)\mathrm{g}_i. \quad (39)$$

And the solution of the above equation is

$$\mathrm{g}_i(\xi)=\mathrm{L}_i^{Pe/2}(\xi) \text{ and } \mathrm{i}=(\lambda_i-1)=0,\ 1,\ 2,\ \cdots, \quad (40)$$

where $\mathrm{L}_i^{Pe/2}(\xi)$ is the associated Laguerre polynomials [11]. Therefore the exact solution of Θ can be written as

$$\Theta(\xi)=\exp(-\xi)\xi^{Pe/2}\sum_{i=0}^{\infty}\mathrm{A}_i\alpha_i\mathrm{L}_i^{Pe/2}(\xi), \quad (41)$$

To meet the orthonormality of f_i's, i.e., $\int_0^{\infty}\mathrm{f}_i(\xi)\mathrm{f}_j(\xi)\mathrm{w}(\xi)\mathrm{d}\xi=\delta_{ij}$, the normalization factors α_i are determined as

$$\alpha_i[\Gamma(\mathrm{i}+1)/\Gamma(\mathrm{i}+\mathrm{Pe}/2+1)]^{1/2}. \quad (42)$$

It is assumed that $\Psi(\xi)$ can be expressed as

$$\Psi(\xi)=\sum_{i=0}^{\infty}\mathrm{A}_i\psi_i(\xi), \quad (43)$$

where ψ_i are obtained by solving

$$\xi\frac{\mathrm{d}^2\psi_i}{\mathrm{d}\xi^2}+\left(1-\frac{\mathrm{R}}{\Gamma(\mathrm{Pe}/2)}\xi^{(Pe/2-1)}\exp(-\xi)\xi\right)\frac{\mathrm{d}\psi_i}{\mathrm{d}\xi}-\frac{\mathrm{n}^2}{4\xi}\psi_i=-\mathrm{R}\frac{\mathrm{n}^2}{4\xi}\alpha_i\exp(-\xi)\xi^{Pe/2}\mathrm{L}_i^{Pe/2}(\xi). \quad (44)$$

However, ψ_i cannot be expressed in a closed form. By substituting $\Psi(\xi)$ and $\Theta(\xi)$ into Eq. (31) and using the orthogonality of $\mathrm{L}_i^{Pe/2}(\xi)$'s, Eq. (31) can be rewritten in the following matrix form:

$$\sigma\mathbf{a}=\mathbf{B}\mathbf{a}, \tag{45}$$

where

$$B_{i,j}=-\lambda_{i-1}\delta_{i-1,j-1}-\frac{n^2}{4}D_{i-1,j-1}+\frac{1}{2}PeG_{i-1,j-1},$$

$$D_{i,j}=\alpha_i\alpha_j\int_0^\infty L_i^{Pe/2}(\xi)L_j^{Pe/2}(\xi)\xi^{-1}p(\xi)d\xi$$

$$=\alpha_i\alpha_j\sum_{k=0}^{i\le j}\Gamma(k+Pe/2+1)/\Gamma(k+1)$$

$$G_{i,j}=\alpha_j\int_0^\infty-\frac{d\theta_0}{d\xi}\psi_i(\xi)L_j^{Pe/2}(\xi)d\xi$$

$$=\alpha_j\frac{1}{\Gamma(Pe/2)}\int_0^\infty\xi^{-1}p(\xi)\psi_i(\xi)L_j^{Pe/2}(\xi)d\xi,$$

$$\mathbf{a}=[A_0,A_1,A_3,\cdots,A_n]^T,$$

wherein $p(\xi)=\exp(-\xi)\xi^{Pe/2}$ is the weighting function and δ_{mn} is Kronecker's delta. The above equation gives important information on the effects of conduction, convection and viscosity gradient. The conduction terms $-\lambda_{i-1}d_{i-1,j-1}-(n^2/4)D_{i-1,j-1}$ make the system stable, whereas the convective term $(1/2)PeRn^2G_{i-1,j-1}$ has the opposite effect on the stability. And, therefore there might exist the neutral stability condition where two opposite effects are in equilibrium. Here, the neutral stability condition is determined by setting the maximum value of the eigenvalue of the matrix **B** to 0. Since the convective term $(1/2)PeRn^2G_{i-1,j-1}$ cannot be expressed in a closed form, it should be obtained through numerical integration.

For high Pe and finite R, from Eq. (34), Θ can be expressed as

$$\Theta(\eta)=\sum_{i=0}^{\infty}\bar{A}_i\bar{f}_i(\eta), \tag{46}$$

where $\bar{f}_i(\eta)$ is the eigenfunction of the following Sturm-Liouville equation

$$\frac{d^2\bar{f}_i}{\partial\eta^2}+2\eta\frac{d\bar{f}_i}{d\eta}=-\lambda_i\bar{f}_i, \tag{47}$$

Now, $\bar{f}_i(\eta)$ will be pursued in the following form:

$$\bar{f}_i(\eta)=\bar{\alpha}_i\exp(-\eta^2)\bar{g}_i(\eta). \tag{48}$$

By substituting the above form into Eq. (47), the following equation is obtained:

$$\frac{d^2\bar{g}_i}{d\eta^2}-2\eta\frac{d\bar{g}_i}{d\eta}=-(\bar{\lambda}_i-2)\bar{g}_i. \tag{49}$$

And the solution of the above equation is

$$\bar{g}_i(\eta)=H_i(\eta)\ \text{ and }\ i=(\bar{\lambda}_i-2)=0,1,2,\cdots, \tag{50}$$

where $H_i(\eta)$'s are the Hermite polynomials [11]. $\bar{\alpha}_i$ can be determined by using the orthogonality of $\bar{f}_i(\eta)$'s as

$$\bar{\alpha}_i=[\sqrt{\pi}\Gamma(i+1)2^i]^{-1/2}. \tag{51}$$

Therefore, the exact solution of Θ can be written as

$$\Theta(\eta)=\exp(-\eta^2)\sum_{i=0}^{\infty}\bar{A}_i\bar{\alpha}_iH_i(\eta), \tag{52}$$

where the undetermined coefficients A_i can be determined by using the orthogonality of $H_i(\eta)$'s.

It is assumed the $\Psi^*(\eta)$ can be expressed as

$$\Psi^*(\eta)=R^*a^2\sum_{i=0}^{\infty}\bar{A}_i\alpha_i\bar{\psi}_i(\eta), \tag{53}$$

where ψ_i can be obtained by solving

$$D^2\bar{\psi}_i+\frac{R}{\sqrt{\pi}}\exp(-\eta^2)D\bar{\psi}_i-a^2\bar{\psi}_i=\exp(-\eta^2)H_i(\eta), \tag{54}$$

where $D=d/d\eta$. For the extreme case where $Pe\to\infty$ and $R\to0$ but $R^*(=R\sqrt{Pe})$ has a finite value, Eq. (54) is reduced as

$$\left(\frac{d^2}{d\eta^2}-a^2\right)\bar{\psi}_i=\exp(-\eta^2)H_i(\eta), \tag{55}$$

and $\bar{\psi}_i$ can be solved analytically as

$$\bar{\psi}_i=\frac{-1}{2a}\left[\exp(a\eta)\left\{\int_\eta^\infty\exp(-a^*\zeta-\zeta^2)H_i(\zeta)d\zeta\right\}\right.$$
$$\left.+\exp(-a\eta)\left\{\int_{-\infty}^{\eta}\exp(a\zeta-\zeta^2)H_i(\zeta)d\zeta\right\}\right] \tag{56}$$

By applying the similar procedure which is employed to obtain Eq. (45), the stability equation is approximated as

$$\sigma\bar{\mathbf{a}}=\bar{\mathbf{B}}\bar{\mathbf{a}}, \tag{57}$$

where

$$\bar{B}_{i,j}=-\frac{1}{2}(\bar{\lambda}_{i-1}+a^2)\delta_{ij}+\frac{1}{2}\frac{R^*a^2}{\sqrt{\pi}}\bar{G}_{i-1,j-1},$$

$$\bar{G}_{i-1,j-1}=\int_{-\infty}^{\infty}\bar{f}_{i-1}(\eta)\bar{\psi}_{j-1}(\eta)d\xi,$$

$$\bar{\mathbf{a}}=[\bar{A}_0,\bar{A}_1,\bar{A}_2,\cdots,\bar{A}_n]^T$$

$$\mathbf{y}=[\bar{A}_0,\bar{A}_1,\bar{A}_2,\cdots,\bar{A}_n]^T.$$

2. Numerical Shooting Method

Since the velocity disturbance field cannot be obtained analytically except for the limiting case of large Pe and small R, a fully analytic solution is possible only for the limiting case of $Pe\to\infty$ and $R\to0$ but finite $R^*(=R\sqrt{Pe})$. Therefore, the above spectral analysis has its own limit even though it can give the exact solution. Now, the stability Eqs. (30)-(32) are tried to be solved with the numerical shooting method [12-14].

To integrate the stability Eqs. (30)-(32), a trial value of the eigenvalue σ and the values of $d\Psi/d\xi$ Θ and $d\Theta/d\xi$ at $\xi=\sqrt{Pe}$ are assumed properly for given R, n and Pe. Since the boundary conditions (32) are all homogeneous, the value of Ψ at $\xi=\sqrt{Pe}$ can be assigned arbitrarily. This procedure is based on the shooting method in which the boundary value problem is transformed into the initial value problem. The trial values at $\xi=\sqrt{Pe}$ give all the information to make numerical integration smooth. Integration based on the 4th-order Runge-Kutta method is performed from the displacing front, $\xi=\sqrt{Pe}$, to the injection center, $\xi=0$, and to the fictitious outer boundary satisfying the infinite boundary conditions. By using the Newton-Raphson iteration, the trial values σ, $d\Psi/d\xi$, Θ and $d\Theta/d\xi$ at $\xi=\sqrt{Pe}$ are corrected until the stability equations satisfy the boundary conditions (32) within the relative tolerance of 10^{-10}. Then, by increasing the fictitious outer boundary step by step, the above integration is repeated. Finally, the value of is decided through the extrapolation. For the large Pe case, the similar solution procedure is applied

to stability Eqs. (33)-(35).

RESULTS AND DISCUSSION

For the limiting case of n=0, the growth rate can be calculated analytically. In this limiting case, to meet Eq. (44) under the boundary condition (32), Ψ=0 should be satisfied. Therefore, the characteristic matrix in Eq. (45) is reduced as

$$B_{i,j}=-\lambda_{i-1}\delta_{i-1,j-1}, \tag{58}$$

and therefore, the growth rate σ should be

$$\sigma=-\lambda_0=-1. \tag{59}$$

Recently, based on the spectral approach, Pritchard [9] expanded $\Phi(\tau,\xi)$ as

$$\Theta(\tau,\xi)=\exp(-\xi)\xi^{Pe/2}\sum_{j=0}^{\infty}A_j(\tau)\tau^{-1-j}L_j^{Pe/2}(\xi), \tag{60}$$

rather than the present (41). However, this spectral expansion needs a mathematical justification for the incursion of a factor τ^{-i-j} and suffers from a severe singularity when $\tau\to 0$. For the limiting case of n$\to$0, he showed that the dominant mode of instability is

$$\Theta(\tau,\xi)=A_0(\tau)\tau^{-1}L_0^{Pe/2}(\xi)\exp(-\xi)\xi^{Pe/2}, \tag{61}$$

and the corresponding growth rate is

$$\frac{1}{A_0}\frac{dA_0}{d\tau}=0 \text{ for } n\to 0. \tag{62}$$

Pritchard's growth constant can be rewritten as, in the present definition of the growth rate,

$$\sigma=-1 \text{ for } n\to 0, \tag{63}$$

since $\sigma=\tau(1/A_0)(dA_0/d\tau)-1$ from Eqs. (29) and (62).

Another limiting case of Pe$\to\infty$ and R$\to$0 but finite $R^*(=R\sqrt{Pe})$, the analytically obtained growth rates are summarized in Fig. 3. This figure shows that there exists a critical R_c^*, under which the growth rate is always negative, i.e., the system is unconditionally stable.

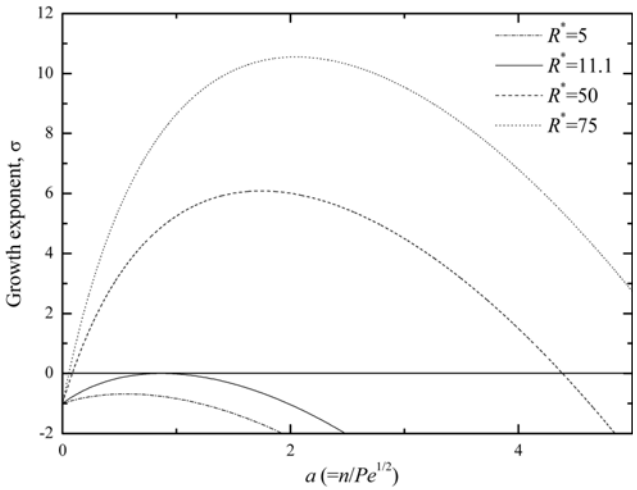

Fig. 3. Growth constants for the various R^* in the limiting case of Pe$\to\infty$. For the region of $R^*<R_c^*$, the growth constant is always negative, i.e. unconditionally stable.

Based on the results summarized in Fig. 3, the neutral stability curves at which σ=0 should be satisfied are calculated and compared in Fig. 4. It is interesting that the second solution is identical with the first order one, and the third-order solution is nearly identical with

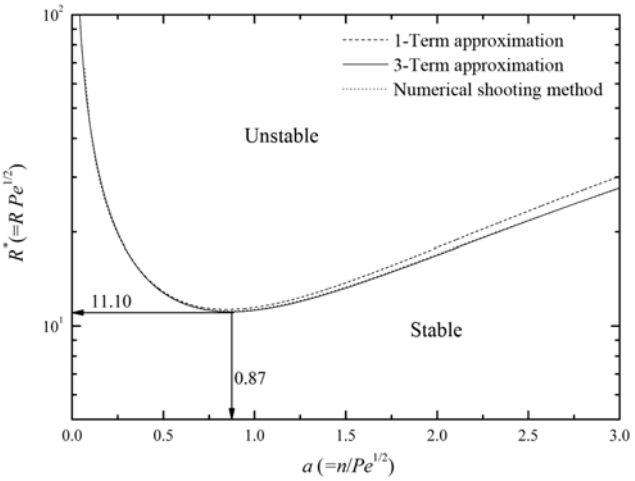

Fig. 4. Neutral stability curve for Pe$\to\infty$. The 2nd order solution is identical with the 1st order one.

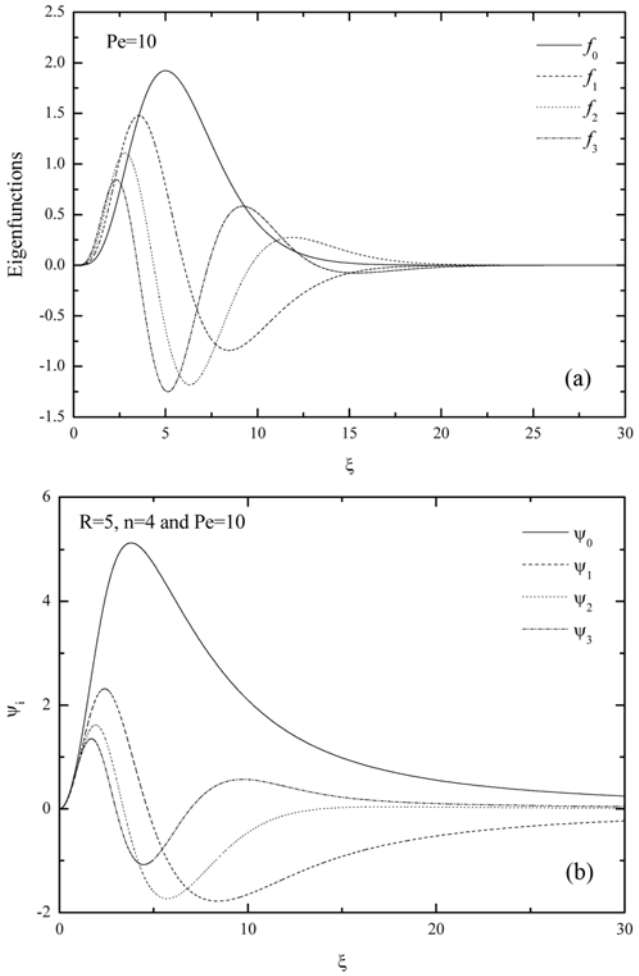

Fig. 5. Eigenfunctions for Pe=10: (a) $f_i(\xi)$ and (b) $\psi_i(\xi)$ for R=5 and n=4.

the numerical solution by using the standard shooting method. Based on the 3-term approximation, their stability limits under Pe→∞ and 0<R<<1 are

$$R_c^*(=R_c\sqrt{Pe})=11.10 \text{ and } a_c(=n_c/\sqrt{Pe})=0.87. \quad (64)$$

This means that for high Pe case, the present system is unstable with respect to the disturbance given in Eq. (28) in the case of $11.10/\sqrt{Pe} \le R_c$.

Except for the above limiting cases, since the closed form of the solution of Eq. (44) or (54) cannot be obtained, a fully analytical approach is not possible. For the specific case of Pe=10, the eigenfunctions $f_i(\xi)$ and $\psi_i(\xi)$ the numerically obtained are summarized in Fig. 5. Based on these eigenfunctions $f_i(\xi)$ and $\psi_i(\xi)$, the calculated growth rate is compares well with the numerical shooting solution in Fig. 6. For a given R, Pe and n, the eigenfunctions ψ can be obtained by solving Eq. (44) and calculating the growth rate σ. However, to find R to satisfy σ=0 for a given Pe and n is not simple since the closed form of the eigenfunctions ψ_i is not known. To avoid this mathematical difficulty, we rely on the numerical shooting method to achieve the neutral stability curve as shown in Fig. 7.

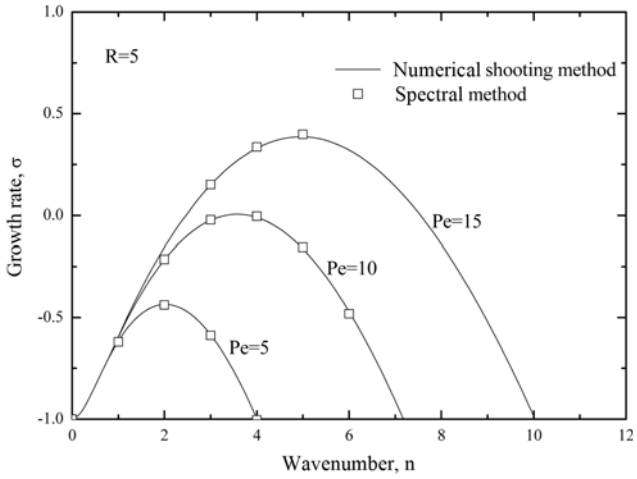

Fig. 6. Comparison of the growth rates obtained from the spectral analysis and the numerical shooting method.

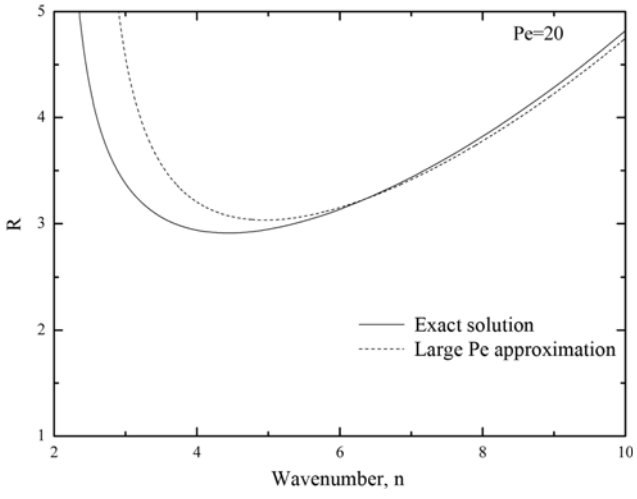

Fig. 7. Comparison of the neutral stability curves obtained from the exact solution and large Pe approximation.

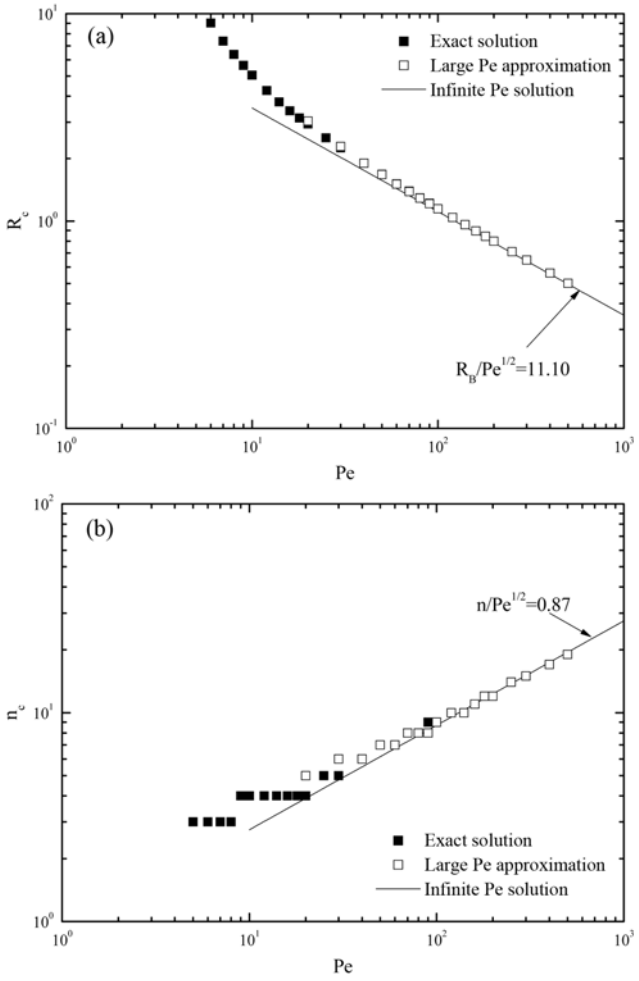

Fig. 8. Comparison of the critical conditions from the various approximations: (a) critical R and (b) critical wavenumber.

As Pe increases, the stiffness of Eqs. (30) and (31) prevents us from obtaining a numerical solution. For the case of Pe≥20, we used large Pe approximation given in Eqs. (33)-(35). For the specific case of Pe=20, the neutral stability curves obtained from the exact solution and the large Pe approximation are compared in Fig. 7. As shown, large Pe approximation gives a quite reasonable solution. The critical conditions which correspond to the minimum of the neutral stability curve are summarized in Fig. 8.

Holloway and de Bruyn [2,3] conducted experimental and numerical simulation work on the onset of the radial viscous fingering in a Hele-Shaw cell. They found that the viscosity contrast M{=exp(R)} to insure the onset of fingering instability is a strong function of the Péclet number as shown in Fig. 14 of Holloway and de Bruyn [3]. They insisted that fingering instability cannot be expected even for the high Pe number system if M_c<20. Even though a direct comparison is not possible, Holloway and de Bruyn's experimental results show nearly 10 times lager viscosity ratio than the present results summarized in Fig. 9. This discrepancy may be caused by the experimental condition where the heat loss through the boundaries is inevitable and, therefore, the viscosity contrast vanishes.

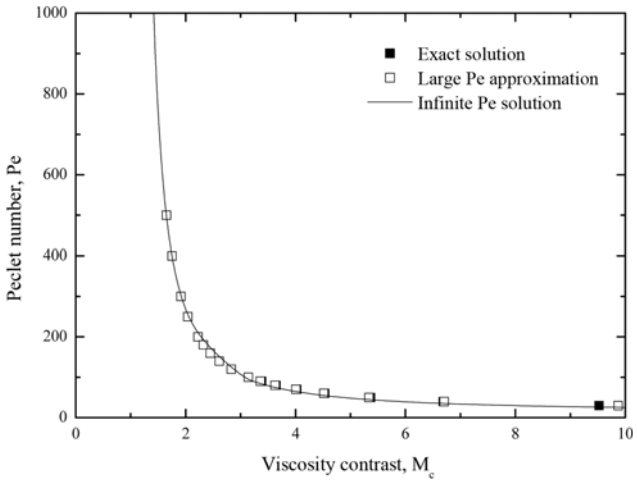

Fig. 9. Comparison of the critical viscosity ratio M_c from the various approximations.

CONCLUSIONS

The critical condition to mark the onset of the fingering motion and its growth has been analyzed by using linear theory. In the self-similar domain, the stability equations have been derived under the normal mode analysis and solved analytically and numerically. Through spectral analysis, the disturbances are expanded as a series of orthogonal functions and the growth rates are obtained by solving a matrix eigenvalue problem. For small Pe system, the growth rates obtained analytically support the numerical shooting solutions. For the case of Pe≥20, the large Pe approximation suggest quite reasonable stability criteria. For the limiting case of $Pe\rightarrow\infty$, n and R were rescaled as $a(=n/\sqrt{Pe})$ and $R^*(=R\sqrt{Pe})$ and the critical values a_c and R_c^* were obtained analytically. For Pe≥100, this limiting case explains the system quite well. The present spectral analysis and numerical shooting method can be used to study the similar stability problem.

REFERENCES

1. S. Hill, *Chem. Eng. Sci*., **1**, 247 (1952).
2. K. E. Holloway and J. R. de Bruyn, *Can. J. Phys*., **83**, 551 (2005).
3. K. E. Holloway and J. R. de Bruyn, *Can. J. Phys.*, **84**, 274 (2006).
4. C. T. Tan and G. M. Homsy, *Phys. Fluids*, **30**, 1239 (1987).
5. Y. C. Yortsos, *Phys. Fluids*, **30**, 2928 (1987).
6. A. Riaz and E. Meiburg, *Phys. Fluids*, **15**, 938 (2003).
7. A. Riaz and E. Meiburg, *J. Fluid Mech*., **494**, 95 (2003).
8. A. Riaz, C. Pankiewitz and E. Meiburg, *Phys. Fluids*, **16**, 3592 (2004).
9. D. Pritchard, *J. Fluid Mech*., **508**, 133 (2004).
10. M. C. Kim, *Z. Angew. Math. Phys.*, DOI:10.1007/s00033-011-0182-8.
11. M. Abramowitz and I. A. Stegun, *Handbook of mathematical functions with formulas, graphs, and mathematical tables*, New York, Dover Publications (1972).
12. I. G. Hwang and M. C. Kim, *Korean J. Chem. Eng*., **28**, 697 (2011).
13. I. G. Hwang and C. K. Choi, *Korean J. Chem. Eng*., **25**, 199 (2008).
14. I. G. Hwang and C. K. Choi, *Korean Chem. Eng. Res*., **25**, 644 (1996).